

## Adhesively-bonded Patch Repair with Composites

P.C. Pandey and S. Kumar\*

*Indian Institute of Science, Bangalore-560 012*

*\*E-mail: kumar.shanmugam@eng.ox.ac.uk*

### ABSTRACT

Adhesively-bonded composite patch repairs over cracked or corrosion-damaged metallic aircraft structures have shown great promise for extending life of ageing structures. This study presents the numerical investigation into the interface behaviour of adhesively-bonded cracked aluminum alloy substrate patched with fibre-reinforced composite material. The adhesive is modelled as an elasto-plastic bilinear material to characterise the debond behaviour, while the defective substrate is regarded as linear elastic continuum. Two typical patch shapes were selected based on information available in the literature. Geometric and material nonlinear analyses for square and octagonal patches were performed to capture peel and shear stresses developed between the substrate and the patch to examine the possibility of interface delamination/debonding. Parametric studies on adhesive thickness and patch thickness were carried out to predict their influence on damage tolerance of repaired structures.

**Keywords:** Three-dimensional finite elements, adhesively-bonded composite-patch repair, structure life extension, geometric and material nonlinearity

### 1. INTRODUCTION

Bonded patches are used for repair of sandwich panels, cracks in metallic structures, and reinforcement of deficient structures. Composite patching is the most widely used method of restoring the load-carrying capacity of the weakened structure or reinforcing the damaged zone with splice or doubler of a material having strength and stiffness higher than the original material. Due to the rapid growth of aerospace industry, analyses of adhesively-bonded patches to repair cracked structures have been the focus for many years. Most of these studies investigated repaired structures using linear analysis and demonstrated the viability of adhesively-bonded patch-repairs as a means to improve the durability and damage tolerance of cracked metallic structures efficiently and economically<sup>1-6</sup>.

The Aeronautical and Maritime Research Laboratory researched the bonded patch method<sup>7</sup> in the early 1970s. Later on, Baker and Jones<sup>1</sup> performed more intensive research on the method and presented the advantages of a composite material patch used for the cracked metal plate repairing. It was found that the bonded patch method not only reduces the weight but also increases the service life. The bonded patch offers many advantages over a mechanically -fastened doubler, which include improved fatigue behaviour, restored stiffness and strength, reduced corrosion, and easy conformance to complex aerodynamic contours<sup>8,9</sup>. For a defective/cracked structure, adhesively-bonded repair significantly reduces stress intensity factor and, as a result, may retard or eliminate crack growth. Several authors<sup>10,11</sup> showed that in practice

the parameters influencing the performances of bonded composite repairs are the patch and adhesive properties. To increase the durability and damage tolerance, many researchers performed experimental tests and numerical analysis on patched thin plates<sup>12</sup>. Kan and Ratwani<sup>13</sup> and Jones,<sup>14</sup> *et al.* tested patched thick plates.

Adhesively-bonded patch repair assuming linear elastic behaviour was investigated by three-layer technique<sup>15,16</sup>. In this technique, finite element analysis (FEA) used Mindlin plate elements to model the cracked aluminum plate, adhesive and composite patch. The most common adhesives used currently are epoxies, which exhibit elastic-plastic material behaviour in their application. Therefore, the effects of nonlinear material properties of the adhesive on the damage tolerance of the repaired structure are needed. Further, the asymmetric repair of a structure causes out-of-plane bending, which occurs because of the shift in the neutral axis of the structure under mechanical loading and also because of the mismatch between the coefficients of thermal expansion of the cracked plate and the composite patch<sup>15,16</sup>. This out-of-plane bending could lead to large deflections, which could impose a large displacement on the repaired structure. Hence, geometrically nonlinear analysis is also needed to examine the effects of the out-of-plane bending on the damage tolerance of the repaired structure.

A two-dimensional FEA of adhesively-bonded composite patch repair, considering geometric, and material nonlinearity was carried out to investigate the effects of these nonlinearities on the damage tolerance of the repaired structure<sup>17</sup>. Paul

and Jones<sup>18</sup> of experimental results revealed in that the bonded boron-epoxy repaired aluminum alloy (7075-T6) specimens could provide a 15-time increase in life expectancy. In this study, the interface behaviour of pre-cracked *Al* 2024-T3 substrates with bonded carbon-epoxy patches have been investigated numerically.

**2. FINITE ELEMENT MODELLING**

The substrate and patch were considered to be linear elastic continuum while the adhesive was regarded as bi-linear elasto-plastic material. The elements of composite patch, adhesive layer, and substrate were connected appropriately by merging the nodes in the contact surfaces. The mesh was properly graded in the vicinity of defect so as to capture the steep stress gradients. The analysis considered large deformations and rotations due to out-of-plane bending associated with one-sided patch. The 3-D FEA were carried out using ANSYS Code Version 8.1.

**2.1 Square-patch Geometry**

The geometric configuration of the crack-patch system used in this study was the same as that used by Dillard<sup>19</sup>, which consisted of aluminum alloy (2023-T3) cracked substrate patched with HT145/RS1222 fibre-reinforced composite material and had a lay-up of [0/90/90/0/0/90/90/0/0/90]. The 3-D physical model of the square crack-patch system is shown in Fig. 1. One-fourth of the crack-patch geometry was modelled exploiting double symmetry. One-fourth FE model of the square crack-patch system with necessary boundary conditions is shown in Fig. 2. The substrate and adhesive layer consisted of 3996 brick elements and the patch composed of 360-layered elements. Three and two elements were used across the thickness of the substrate and adhesive layer respectively.

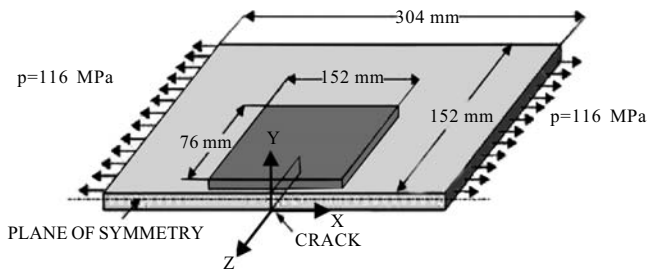


**Figure 1. Three-dimensional physical model of square crack-patch geometry.**

Table 1 shows the geometric and material properties of the crack-patch system. The yield stress and tangent modulus of adhesive are 30 MPa and 1500 MPa, respectively.

**Table 1. Elastic properties of adhesive, substrate, and patch**

Item	Material	Thickness (mm)	Young's modulus <i>E</i> (MPa)	Poisson's ratio $\nu$
Adherend	2024-T3 <i>Al</i> alloy	2.30	7170	0.30
Adhesive	Epoxy	0.23	2220	0.40
Patch	Carbon-epoxy tape	1.00	Composite	Composite

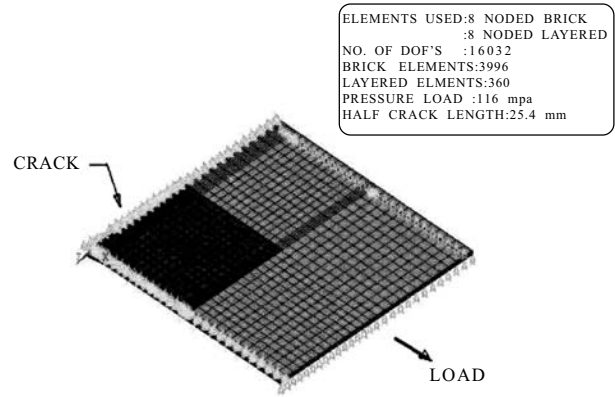


**Figure 2. One fourth finite element model of square crack-patch geometry.**

The elastic properties of composite patch are:  $E_x = 153.8 \text{ GPa}$ ,  $E_y = E_z = 9.96 \text{ GPa}$ ,  $G_{xy} = G_{xz} = 7.39 \text{ GPa}$ ,  $G_{yz} = 4.94 \text{ GPa}$ ,  $\nu_{xy} = \nu_{xz} = 0.168$ , and  $\nu_{yz} = 0.035$ .

**2.2 Octagonal-patch Geometry**

The optimum proportions of the octagonal patch identified by Hart-Smith<sup>20</sup>, was used in this investigation. Materials used were the same as these of square crack-patch system. The HT145/RS1222 fibre-reinforced composite patch has the [0/90/90/0/0/90/90/0/0/90/90/0/0/90] lay-up. The thickness of the substrate, adhesive layer, and patch of octagonal crack-patch system used for both linear and nonlinear analyses were 1.5 mm, 0.2 mm, and 1.4 mm, respectively. One-fourth FE models of different mesh density with physical dimensions are shown in Figs 3 and 4. The FE model (Fig. 4) has 9468 DOFs.

**3. RESULTS AND DISCUSSION**

**3.1 Linear Static Analysis**

Linear elastic analyses were performed initially for both square crack-patch and octagonal crack-patch systems under a tensile surface traction of 116 MPa and 180 MPa, respectively in the direction perpendicular to the plane of crack. The deformed geometry and vonMises equivalent stress of the adhesive material from the linear elastic analyses indicate that the nonlinear analysis considering both geometric nonlinearity and material nonlinearity of the adhesive ought to be performed to accurately predict the state of stress at the crack tips, under the bonded patch, so that any further growth of the crack, that may be possible, can be quantified.

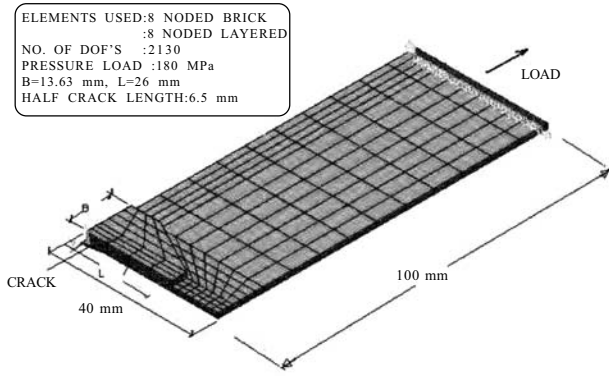
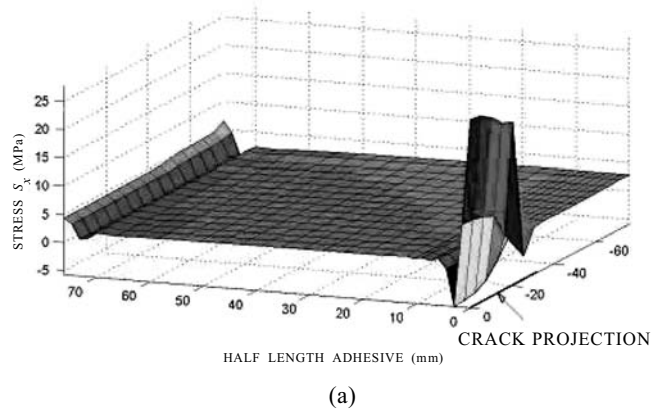


Figure 3. Coarse mesh FE model of octagonal crack-patch system. B and L are dimensions of the patch.



(a)

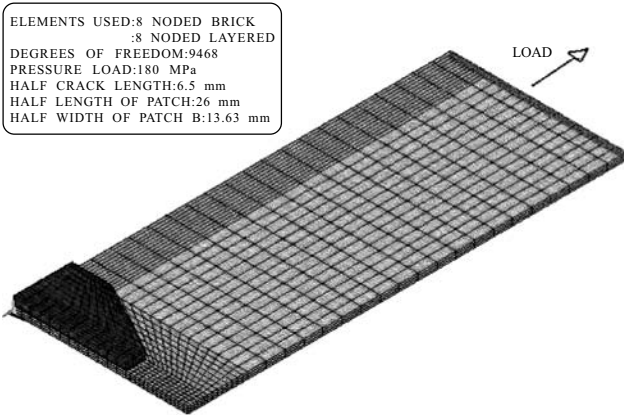
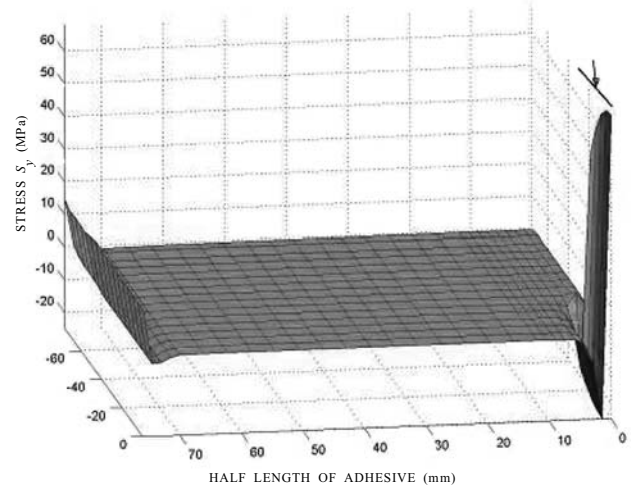


Figure 4. Fine mesh FE model of octagonal crack-patch system.



(b)

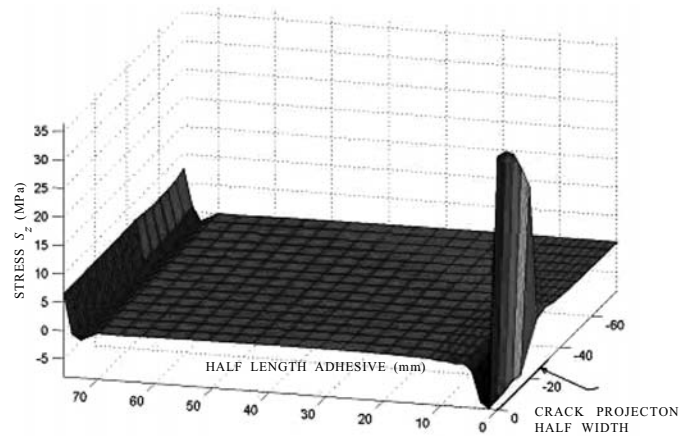
### 3.2 Geometric and Material Nonlinear Static Analysis

#### 3.2.1 Square Crack-patch System

Nonlinear FE analysis of the above system was carried out considering the inelastic behaviour of the adhesive material and large deformations and rotations of the crack-patch system under the same tensile load of 116 MPa. The bondline behaviour was studied by observing the stress distributions at the mid-plane of adhesive layer. Normal components of stress  $S_x$ ,  $S_y$ , and  $S_z$  at the mid-plane of adhesive layer are shown in Figs 5(a), 5(b), and 5(c), respectively. Shear components of stress  $S_{xy}$  and  $S_{yz}$  at the mid-plane of adhesive layer are shown in Figs 6(a) and 6(b), respectively. vonMises equivalent stress  $S_{eq}$  was captured and depicted in Fig.7. It has been observed that the peak shear stresses in the adhesive are at the patch edge. The peel stress  $S_y$  and shear stress  $S_{xy}$  in the adhesive are predominant.

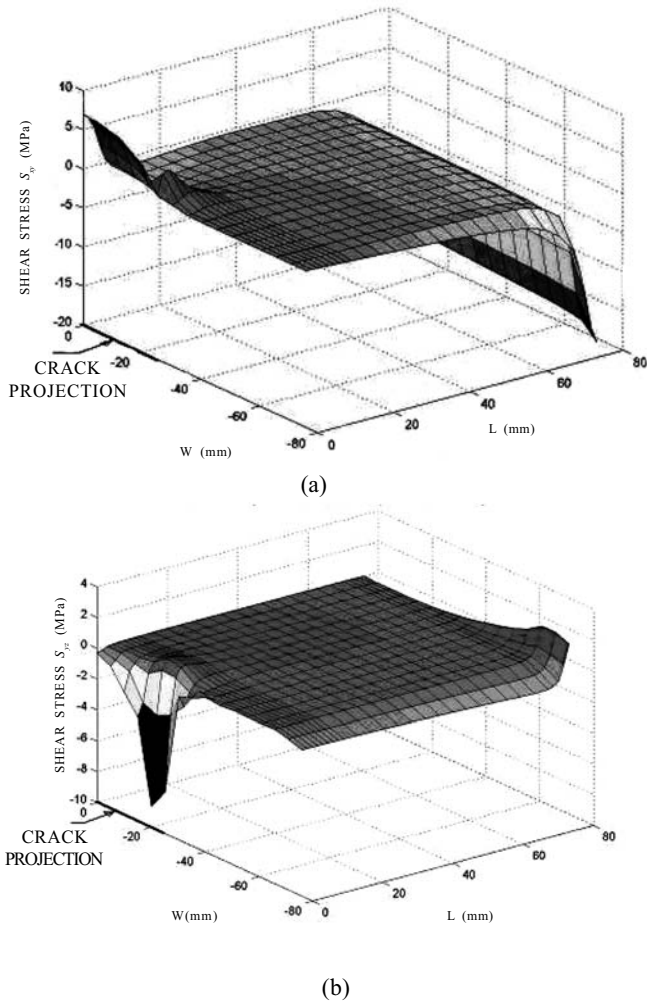
#### 3.2.2 Octagonal Crack-patch System

As was in the previous case, nonlinear (geometric and material) analysis was performed for the octagonal crack-patch system imposing a tensile load of 180 MPa. The adhesive stresses were captured. Normal components of stress  $S_x$ ,  $S_y$ , and  $S_z$  at different sections in the direction

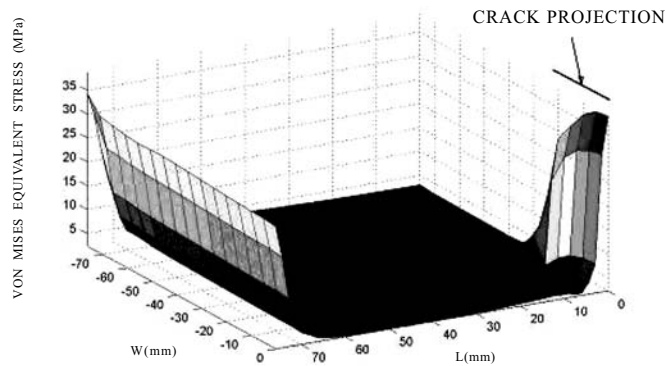


(c)

Figure 5. Geometric and material nonlinear analysis: stress distribution at the mid-plane of adhesive of square crack-patch system: (a) normal stress  $S_x$ , (b) peel stress  $S_y$ , and (c) normal stress  $S_z$ .



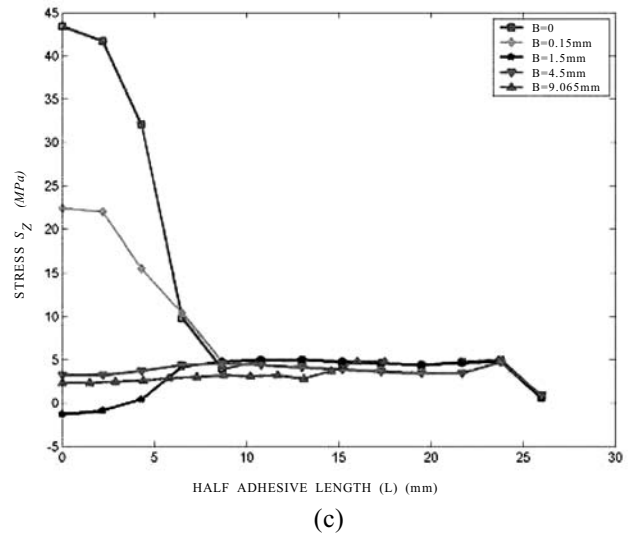
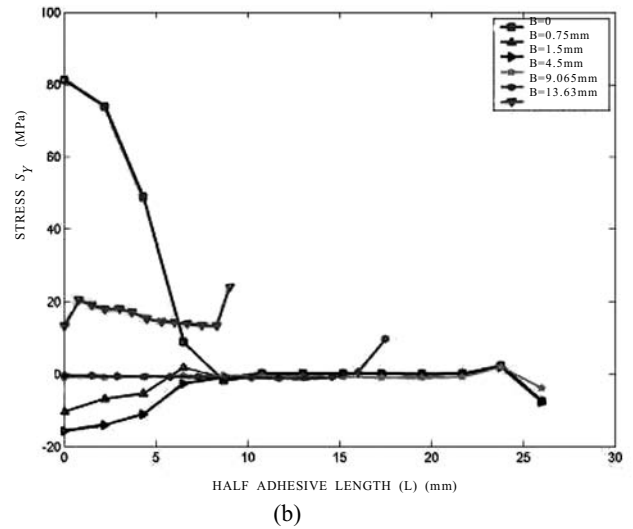
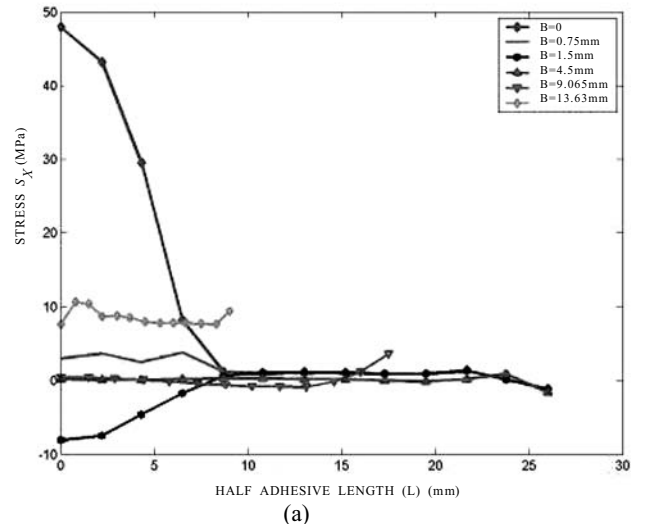
**Figure 6. Geometric and material nonlinear analysis: At the midplane of adhesive of square crack-patch system: (a)  $S_{xy}$  distribution and (b)  $S_{yz}$  distribution.**



**Figure 7. Geometric and material analysis: vonMises equivalent  $S_{eq}$  distribution at the midplane of adhesive of square crack-patch system.**

of B in midplane of adhesive are shown in Figs 8(a) to (d), respectively. B indicates the distance in the direction of patch size B. Shear stress component  $S_{xy}$  at the mid

plane of adhesive layer at different sections of the patch is shown in Fig. 8(d). Peel stress  $S_y$  and shear stress  $S_{xy}$  have been observed to be significant in the vicinity of the crack and also at the patch edge.



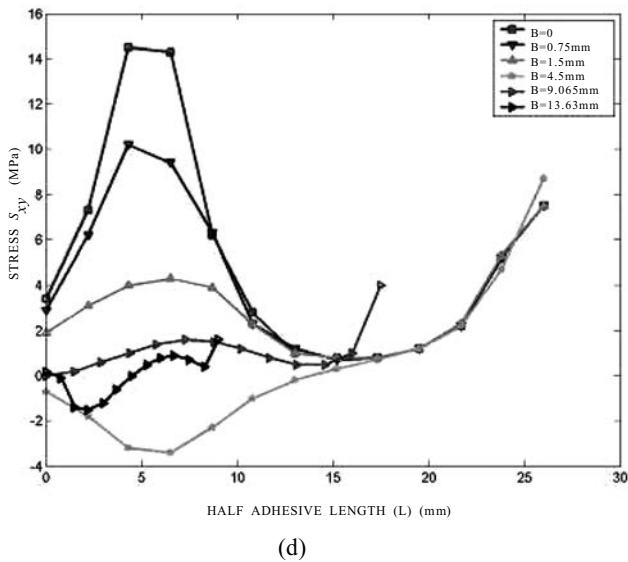


**Figure 8. Geometric and material nonlinear analysis: Stress  $S_{xy}$  distribution at the mid-plane of adhesive at different sections of octagonal crack-patch system: (a) normal stress  $S_x$ , (b) peel stress  $S_y$ , (c) normal stress  $S_z$ , and (d) shear stress  $S_{xy}$  [B indicates the distance in the direction of patch dimension B].**

**3.3 Finite Element Analysis Parametric Studies**

A series of simulated experiments using nonlinear FE analysis were conducted on crack-patch configurations to determine the effects of geometric parameters on strength, damage tolerance, and stiffness. The parametric study consisted of systematically changing the adhesive layer thickness and patch thickness and capturing the stresses and strains. Figure 9 shows the locations of maximum and minimum stresses in the adhesive layers of square and octagonal crack-patch systems.

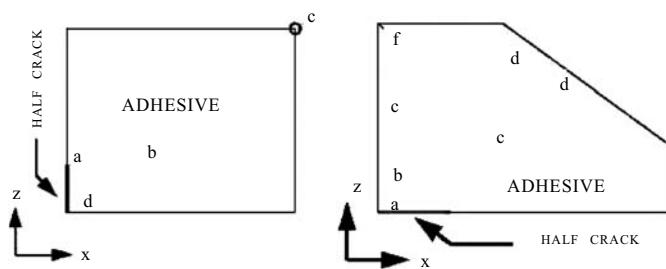


**Figure 9. Locations of maximum and minimum stresses in square and octagonal adhesive layers.**

**3.3.1 Parametric Study of Square Crack-patch System**

The FE simulations were conducted by varying the adhesive layer thickness and patch thickness under a constant tensile load of 116 MPa, to predict the structural response of the interface layer and its influence on the damage tolerance and load carrying capacity. Firstly, adhesive thickness was varied and analyses were performed, keeping substrate and patch thickness constant. Table 2 shows the maximum and minimum stresses and strains in the adhesive layer

with their locations obtained from the elasto-plastic analysis considering geometric nonlinearity for different adhesive thickness and for a given load, substrate thickness, and patch thickness. Secondly, patch thickness was varied, keeping other parameters constant. Table 3 shows the stresses and strains in the adhesive layer with their locations obtained from nonlinear analyses for different patch thickness under the same load of 116 MPa. The FEA indicates that as the thickness of the adhesive increases, other geometric parameters being constant, the normal stress  $S_x$ , normal stress  $S_z$ , shear stress  $S_{xy}$ , vonMises equivalent stress  $S_{eq}$  and equivalent plastic strain  $E_{eq}$  in critical location of the adhesive layer decrease, as can be seen from Figs 10(a) to 10(e), respectively. The equivalent plastic strain in the critical element of the adhesive layer also decreases as thickness of adhesive increases, simulating plain strain condition in the layer. As the patch thickness increases, keeping thickness of the adhesive constant, for the same load, the maximum normal stresses  $S_x$ ,  $S_y$  and  $S_z$  in the adhesive increase up to a particular value and then decrease slowly, and are shown in Figs 11(a), 11(b), and 11(c), respectively. Maximum magnitude of shear stress vonMises equivalent stress  $S_{eq}$ , and equivalent plastic strain  $E_{eq}$  in the adhesive increase with increase of patch thickness. The  $S_{xy}$  variation as a function of patch thickness is shown in Fig. 12.

**3.3.2 Parametric Study of Octagonal Crack-patch System**

Nonlinear analyses octagonal crack-patch system were carried out by varying the adhesive thickness and patch thickness under a constant load of 180 MPa and the stresses and strains at the critical locations of the adhesive layer were captured and listed in Tables 4 and 5, respectively. Increase in adhesive thickness increases the normal stress components  $S_x$ ,  $S_y$  and  $S_z$  as shown in Fig. 13. Shear stress components  $S_{xy}$ ,  $S_{yz}$  and  $S_{zx}$  variation with adhesive thickness, are depicted in Fig. 14. VonMises equivalent stress and equivalent plastic strain in the adhesive layer vary with adhesive thickness as shown in Figs 15(a) and 15(b), respectively. Normal stress components ( $S_x$ ,  $S_y$  and  $S_z$ ) variation in a critical element of adhesive as a function of patch thickness is shown in Fig. 16. Shear stress components ( $S_{xy}$ ,  $S_{yz}$  and  $S_{zx}$ ) in the critical locations of adhesive vary, as shown in Fig. 17 with increase of patch thickness. The variation of equivalent plastic strain in a critical element of the adhesive as a function of patch thickness is shown in Fig. 18.

**4. CONCLUSIONS**

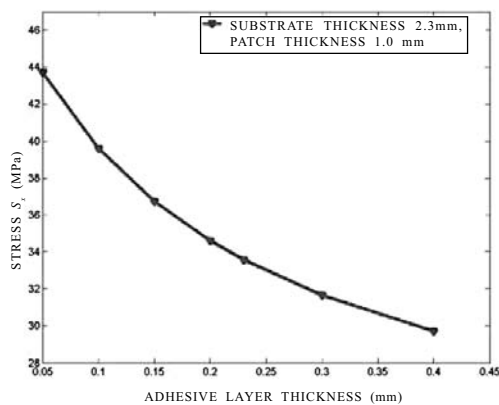
Nonlinear computational analyses of square crack-patch and octagonal crack-patch systems have been performed considering geometric and material nonlinearity under static loading conditions. It has been observed that the peel and shear stresses are predominant and the peak shear stress occurs at the edge of the patch in the adhesive. Different stress and strain-based failure criteria were considered in this study to predict the strength. The position of predicted

**Table 2. Linear (LS) and nonlinear (EP) analysis of square crack-patch system**

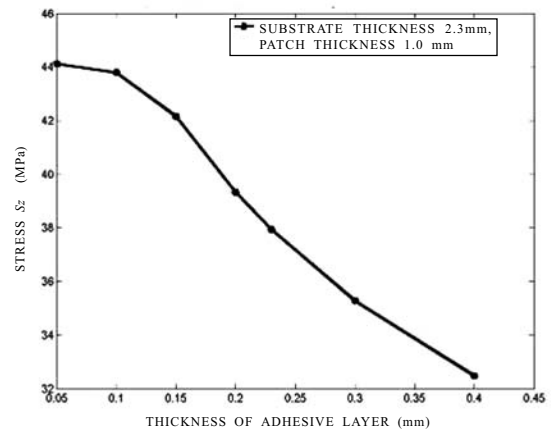
Analysis	Square patch Adhesive thickness (mm)	Maximum and minimum magnitude of stress (MPa)							
		$S_x$	$S_y$	$S_z$	$S_{xy}$	$S_{yz}$	$S_{zx}$	$S_{eq}$	$\epsilon_{eq}^p$
LS	0.23	43.205a	94.819a	50.610 a	13.650a	4.045c	0.116b	57.260a	
		19.211d	-51.769d	-31.157d	-21.225c	-13.991a	-1.426a	1.670d	
	0.05	43.693a	78.564a	44.116a	9.108a	3.431c	0.089b	54.900c	0.005282c
		-18.920d	52.294d	-31.324d	-30.741c	-14.732a	-0.873a	1.915d	
	0.1	39.587a	82.502a	43.787a	8.649a	0.920b	2.913c	47.086c	0.003174c
		-18.564d	-56.294d	-31.536d	-25.275c	-0.927a	-12.731a	2.052d	
0.15	36.721a	78.384a	42.158a	9.0899a	2.614c	0.094b	44.545a	0.002103c	
	-16.095d	-47.814d	-27.178d	-22.395c	-11.453a	-0.972637a	1.876d		
0.20	34.597a	72.025a	39.333a	9.423a	2.417c	0.096b	42.043a	0.001427c	
	-14.051d	-41.848d	-23.848d	-20.584c	-10.5499a	-1.008a	1.761d		
EP	0.23	33.566a	68.889a	37.931a	9.471a	2.798c	0.097b	40.044a	0.001126c
		-12.977d	-38.364d	-22.183d	-19.771c	-10.117a	-1.025a	1.788b	
	0.30	31.650a	62.978a	35.274a	9.487a	2.559c	0.100b	36.381a	0.586e-3c
		-10.825d	-32.485d	-18.996d	-18.291c	-9.32a	-1.061a	1.716d	
	0.40	29.700a	56.782a	32.469a	9.377a	2.305c	0.105b	32.67a	0.111e-3c
		-8.392d	-26.344d	-15.595d	-17.917c	-8.497a	-1.101a	1.832d	

**Table 3. Geometric and material nonlinear (EP) analysis of square crack-patch system**

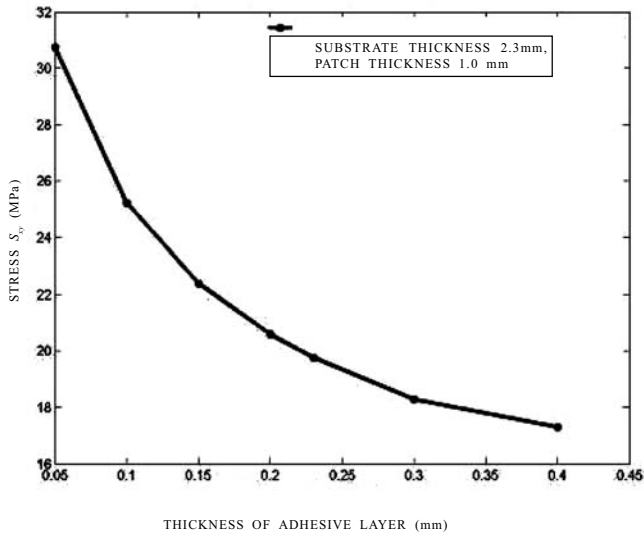
Case	Square patch Patch thickness (mm)	N	Maximum and minimum magnitude of stress (MPa)							
			$S_x$	$S_y$	$S_z$	$S_{xy}$	$S_{yz}$	$S_{zx}$	$S_{eq}$	$\epsilon_{eq}^p$
EP	0.4	4	28.395a	47.381a	25.139a	15.603a	1.035b	0.1712b	38.657a	0.774e-3a'
			-11.00d	-39.424d	-22.526d	-13.304c	-9.551a	-1.641a	2.448e	
	0.8	8	32.032a	67.165a	36.359a	11.52a	2.269c	0.1140b	40.955a	0.441e-3c
			-12.851d	-41.324d	-23.561d	-18.064c	-10.321a	-1.181a	2.052d	
	1.0	10	33.566a	68.889a	37.931a	9.471a	2.798c	0.097b	40.044c	0.001126c
			-12.977d	-38.364d	-22.183d	-19.771c	-10.117a	-1.025a	1.788b	
	1.6	16	33.002a	67.12a	38.27a	5.148a	3.343c	0.08b	42.401c	0.00263c
			-10.693d	-28.49d	-16.87d	-23.324c	-9.053a	-0.7363a	1.18d	
	2.0	20	32.321a	64.587a	-14.186d	-25.199c	-8.41a	-0.706c	46.238c	0.00344c
			-9.169d	-23.794d	37.364a	763a	3.717c	0.1176b	1.177b	



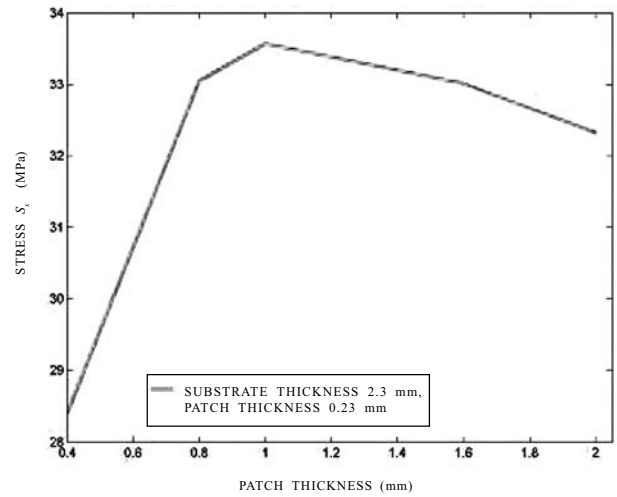
(a)



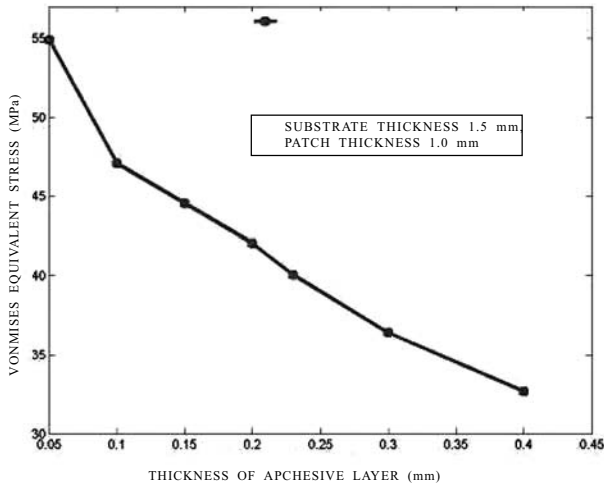
(b)



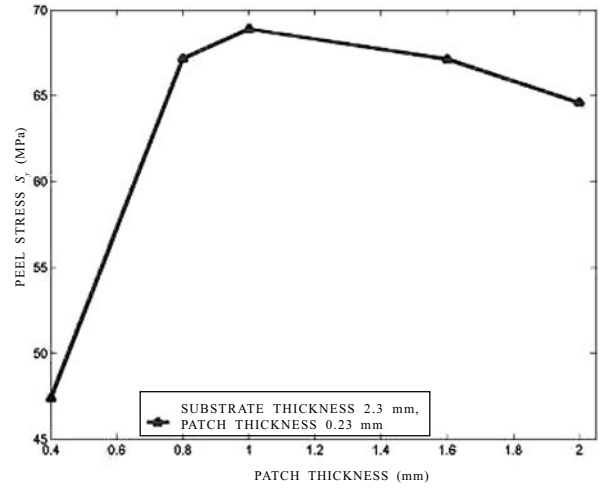
(c)



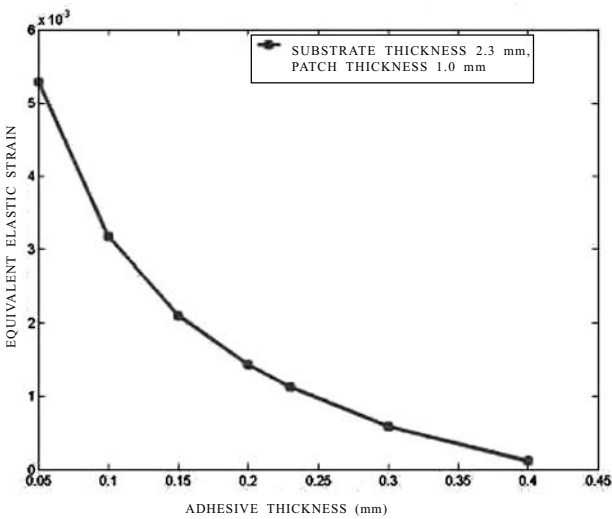
(a)



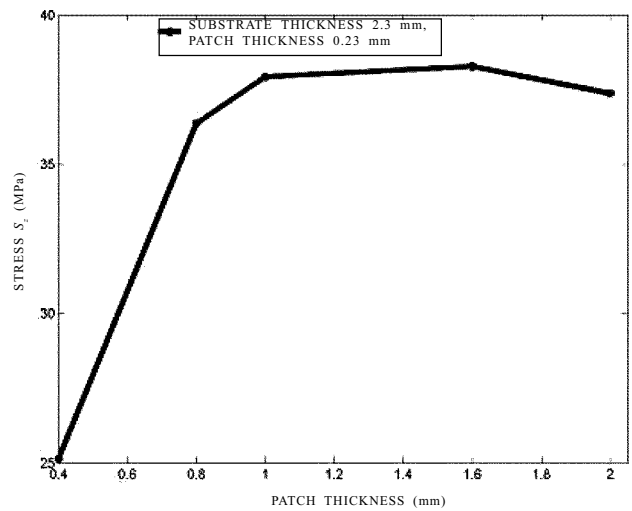
(d)



(b)



(e)



(c)

**Figure 10. Geometric and material nonlinear analysis: A critical location of adhesive in square crack-patch system, the variation of: (a) normal stress  $S_x$ , (b) normal stress  $S_y$ , (c) shear stress  $S_{xy}$ , (d) vonMises equivalent stress  $S_{eq}$ , and (e) equivalent plastic strain  $S_{eq}$ .**

**Figure 11. Geometric and material nonlinear analysis: At a critical location of adhesive with patch thickness in square crack-patch system, the variation of: (a) normal stress  $S_x$ , (b) peel stress  $S_y$ , and (c) normal stress  $S_x$ .**

Table 4. Linear (LS) and nonlinear (EP) analysis of octagonal crack-patch system

Analysis	Octagonal patch Adhesive thickness (mm)	Maximum and minimum magnitude of stress (MPa)							
		$S_x$	$S_y$	$S_z$	$S_{xy}$	$S_{yz}$	$S_{zx}$	$S_{eq}$	$\epsilon_{eq}^p$
LS	0.2	52.789a	87.945a	51.864a	0.187a	20.774d	3.394d	46.767a	-
		-15.508b	-26.082b	-8.056b	-4.046c	-10.03a	-1.749d	1.808e	
	0.05	62.232a	97.827a	58.545a	25.729a	33.077d	2.429d	60.37d	0.006442d
		-34.653b	-59.094b	-22.184b	-8.750c	-10.90c	-1.430d	2.222e	
EP	0.1	52.412a	82.297a	53.498a	20.906a	25.823d	2.3941d	48.291d	0.00388d
		-26.615b	-47.577b	-13.667b	-6.232c	-9.232b	-1.065d	1.866e	
	0.2	49.948a	82.462a	49.897a	16.718a	20.379d	2.922d	40.161a	0.00186d
		-14.789b	-26.1b	-6.822b	-3.962c	-9.1351b	-1.812d	1.856b	
EP	0.3	43.299a	69.613a	46.54a	15.624a	17.59d	2.81 d	36.06a	0.8011e-3d
		-10.938b	-16.804	-5.376b	-2.869c	-8.625b	-1.587d	1.086e	
	0.4	39.035a	61.563a	44.2a	13.586a	-8.123a	-1.544a	1.052e	0.119e-3d
		-9.333b	-16.804b	-3.06b	-2.218c	15.56d	2.715d	31.282a	

Table 5. Geometric and material nonlinear (EP) analysis of octagonal crack-patch system

Case	Octagonal patch Patch thickness (mm)	N	Maximum and minimum magnitude of stress (MPa)									
			$S_x$	$S_y$	$S_z$	$S_{xy}$	$S_{yz}$	$S_{zx}$	$S_{eq}$	$\epsilon_{eq}^p$		
EP	0.4	4	25.079a	44.404a	30.34a	16.311a	17.556f	2.254d	40.296a	0.393e-3		
			-17.926b	-32.414b	-6.396b	-4.284c	-11.69a	-1.487a	2.328eA			
	0.8	8	38.578a	65.922a	40.161a	17.557a	19.567f	2.41d	41.74a	0.914e-3		
			-19.054b	-33.82b	-6.747b	-4.196c	-10.875a	-1.486d	2.073e			
	1.4	14	49.948a	82.462a	49.897a	16.718a	20.379d	2.922d	40.161a	0.00186d		
			-14.789b	-26.1b	-6.822b	-3.962c	-9.1351b	-1.812d	1.856b			
	1.6	16	52.417a	85.935a	52.135a	16.204a	20.995f	2.404d	40.913a	0.00216		
			-13.281b	-23.518b	-7.65b	-3.923c	-8.486a	-1.491d'	1.911e			
			2.0	20	55.922a	90.674a	55.472a	15.803a	21.936d	2.549d	42.154d	0.002578
					-12.919b	-20.924b	-8.451b	-3.866c	-7.377a	-1.504d'	1.847e	

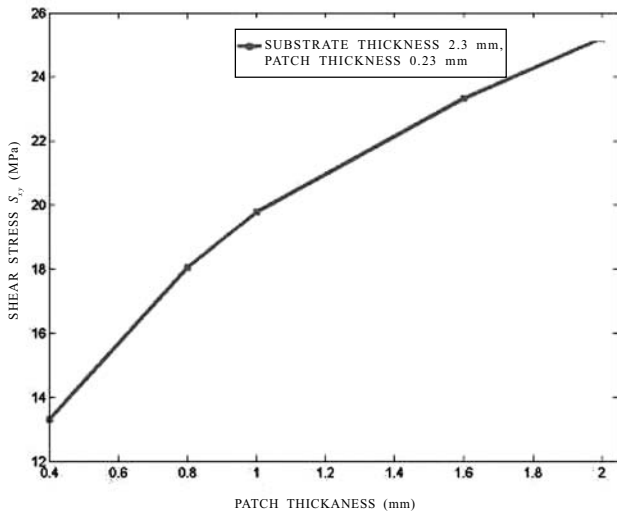


Figure 12. Geometric and material nonlinear analysis: Variation of shear stress  $S_{xy}$  at a critical location of adhesive with patch thickness in square crack-patch system.

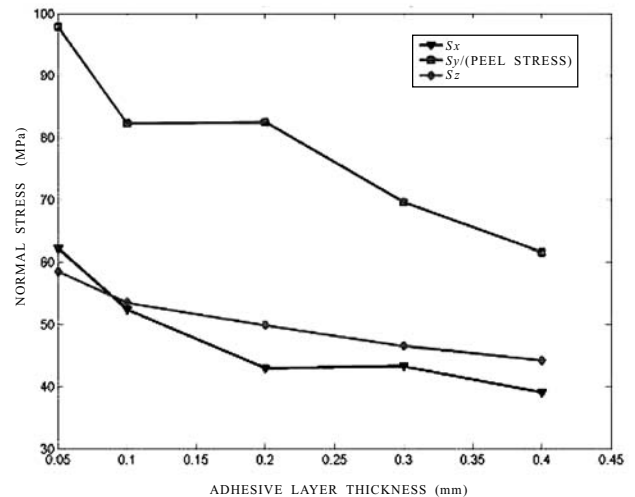


Figure 13. Geometric and material nonlinear analysis: Variation of normal stress components at a critical location of adhesive with adhesive thickness in octagonal crack-patch system.

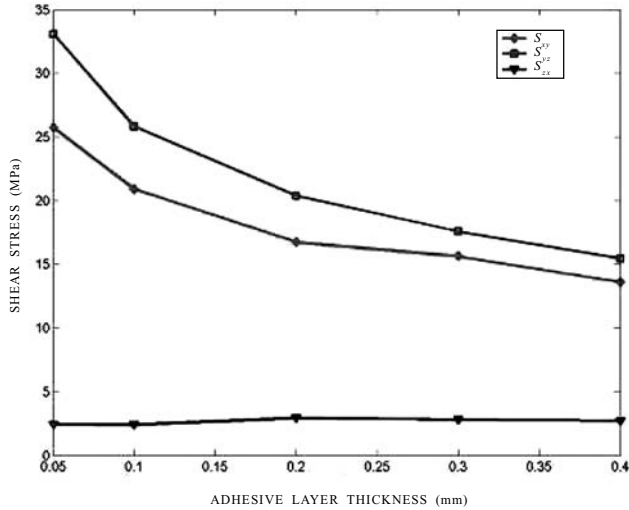


Figure 14. Geometric and material nonlinear analysis: Variation of shear stress components at a critical location of adhesive with adhesive thickness in octagonal crack-patch system.

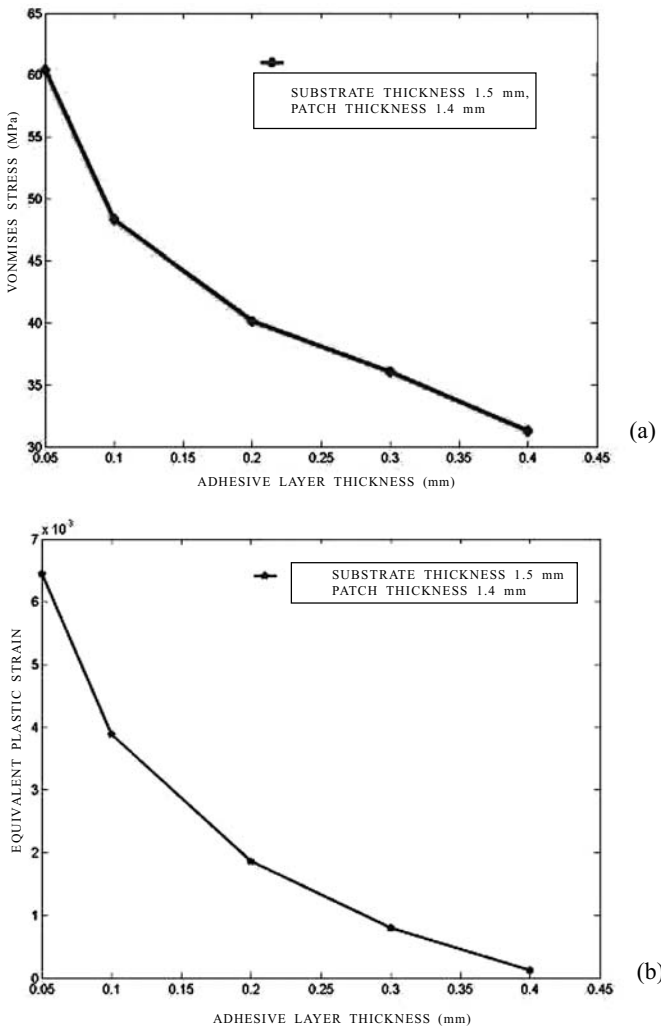


Figure 15. Geometric and material nonlinear analysis: At a critical location of adhesive with adhesive thickness in octagonal crack-patch system, the variation of: (a) vonMises equivalent stress  $S_{eq}$  and (b) equivalent plastic strain.

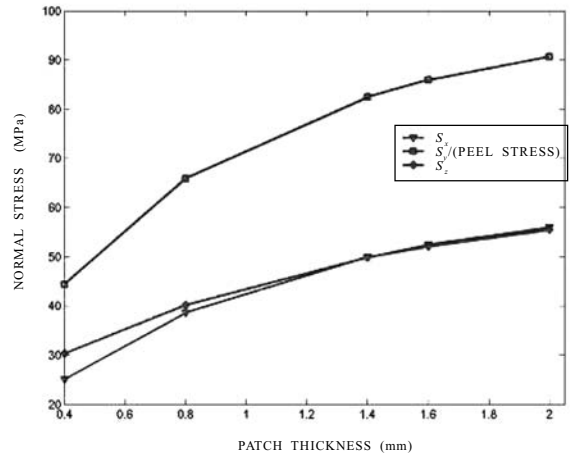


Figure 16. Geometric and material nonlinear analysis: Variation of normal stress components at a critical location of adhesive with patch thickness in octagonal crack-patch system.

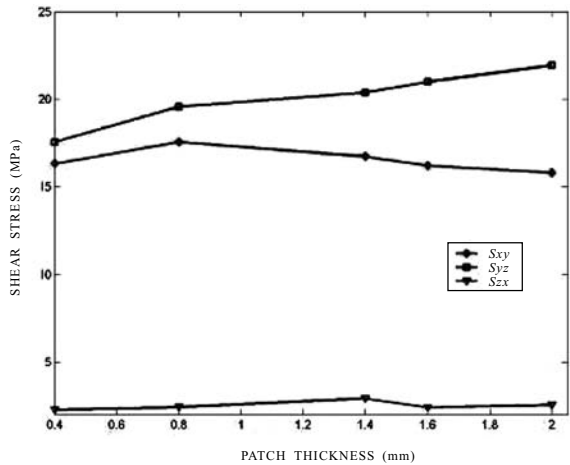


Figure 17. Geometric and material nonlinear analysis: Variation of shear stress components at a critical location of adhesive with patch thickness in octagonal crack-patch system.

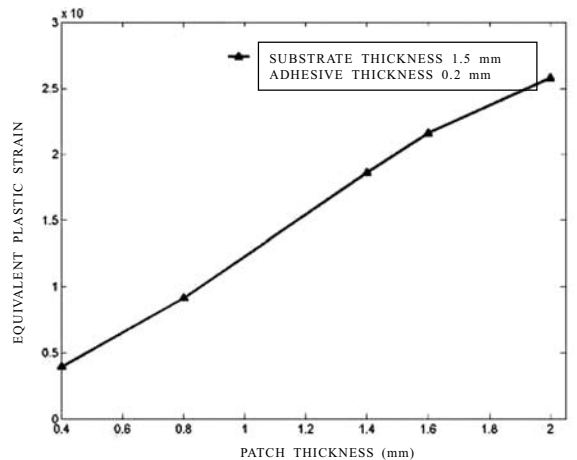


Figure 18. Geometric and material nonlinear analysis: Variation of equivalent plastic strain at a critical location of adhesive with patch thickness in octagonal crack-patch system.

failure in the adhesive has been found to be dependent on failure criteria selected and the crack-patch system geometry. Variably, maximum tensile stress predicts the highest strength of the bonded system. Geometric and material nonlinearity have significant effects on the performance of the crack-patch system. The FE studies indicate that the geometric and material properties of adhesive and patch dictate the mechanical response of the crack-patch system.

**REFERENCES**

1. Baker, A.A. & Jones, R. Bonded repair of aircraft structures. Martinus Nijhoff Publishers, Dordrecht, 1998.
2. Sun, C.T.; Klug, J. & Arendt, C. Analysis of cracked aluminum plates repaired with bonded composite patches. *AIAA Journal*, 1996, **34**(2), 369-74.
3. Pandey, P.C.; *et al.* Nonlinear analysis of adhesively bonded lap joints considering viscoplasticity in adhesives. *Composite Structures*, 1999, **70**(4), 387-13.
4. Pandey, P.C. & Narasimhan, S. Three-dimensional nonlinear analysis of adhesively bonded lap joints considering viscoplasticity in adhesives. *Composite Structures*, 2001, **79**(7), 769-83.
5. Pandey, P.C. & Kumar, S. Three-dimensional nonlinear finite element studies on adhesively bonded patch repairs. ARDB, Govt. of India, 2005. ARDB Project No. DRAO/08/1051165/M/I
6. Kumar, S. Nonlinear finite element study on cyclic-fatigue performance of adhesively bonded joints and structural systems. Faculty of Engineering, Indian Institute of Science. 2005. MSc Thesis.
7. Baker, A.A. Repair efficiency in fatigue-cracked aluminum components reinforced with boron/epoxy patches. *Fatigue Fract. Eng. Mater. Struct.*, 1993, **16**, 753-65.
8. Baker, A.A.; Callinan, R.J.; Davis, M.J.; Jones, R. & Williams, J.G. Repair of Mirage III aircraft using BFRP crack patching technology. *Theo. Appl. Fract. Mech.*, 1984, 1-16.
9. Baker, A.A. Repair of cracked or defective metallic components with advanced fibre composites an overview of Australian work. *Composite Structures*, 1984, **2**, 153-81.
10. Turaga, V.R.S. & Ripudaman, S. Modeling of patch repairs to a thin cracked sheet. *Eng. Fract. Mech.*, 1999, **62**, 267-89.
11. Baker, A.A. Bonded composite repair for fatigue-cracked primary aircraft structure. *Composite Structures*, 1999, **74**, 431-43.
12. Denney, J.J. & Mall, S. Characterization of disbond effects on fatigue crack growth behavior in aluminum plate with bonded composite patch. *Eng. Fract. Mech.*, 1997, **57**, 507-25.
13. Kan, H.P. & Ratwani, M.M. Composite patch repair of thick aluminum structures: Final report. 1983. Airtask No. WF41-400, PE6224. Report No. NADC-82139-60.

United States Navy Air Development Center, Warminster, PA 18974.

14. Jones, R.; Moment L.; Baker, A.A. & Davis, M.J. Bonded repair of metallic components: Thick sections. *Theo. Appl. Fract. Mech.*, 1998, **9**, 61-70.
15. Naboulsi, S. & Mall, S. Modeling of cracked metallic structure with bonded composite patch using three-layer technique. *Composites Structures*, 1996, **35**, 295-08.
16. Naboulsi, S. & Mall, S. Thermal effects on adhesively bonded composite patch repair of cracked aluminum panels. *Theo. Appl. Fract. Mech.*, 1996, **26**, 1-12.
17. Naboulsi, S. & Mall, S. Nonlinear analysis of bonded composite patch repair of cracked aluminum panels. *Composite Structures*, 1998, **41**, 303-13.
18. Paul, J.B. & Jones, R. Bonded composite repair of cracked load bearing holes. *Eng. Fract. Mech.*, 1994, **48**(3), 455-61.
19. David, A. Dillard; *et al.* Two- and three-dimensional geometrical nonlinear finite elements for analysis adhesive joints. *J. Adhesion Adhesives*, **21**, 17-34.
20. Hart-Smith, L.J. Nonlinear closed-form analysis of stresses and defections in bonded one-sided splices and patches. Boeing Report, 1999.

**Contributors**



**Prof P.C. Pandey** obtained his PhD from Liverpool University, UK, in 1979. He was Post Doctoral Fellow in Swansea University. He held Academic Positions at NTU, Singapore and BITS, Pilani before moving to Indian Institute of Science (IISc) in 1988. Currently, he is working as Professor in IISc, Bangalore. His research interests include: linear and nonlinear

FEM, strain space plasticity, continuum damage mechanics, FRP composites, adhesively-bonded joints and integrated force method. He has more than 100 peer reviewed publications to his credit.



**Mr S. Kumar** obtained his BE from College of Engineering, Guindy, Anna University, Chennai in 1999. He worked as Scientist in Gas Turbine research Laboratory (GTRE), Bangalore. He obtained his Masters from IISc Bangalore in 2002. He was awarded Rolls-Royce/DTI Fellowship to work for Rolls-Royce at the University of Southampton, UK in 2005. He was awarded fully funded EPSRC

award at Oxford to pursue DPhil. His research interests include: multiscale modelling, constitutive modelling, computational mechanics, bonded joints and computational materials science.